Eur Biophys J
DOI 10.1007/s00249-010-0616-9

ORIGINAL PAPER

Stiffness of γ subunit of F_1-ATPase

Daichi Okuno · Ryota Iino · Hiroyuki Noji

Received: 29 March 2010 / Revised: 17 May 2010 / Accepted: 26 May 2010

Abstract F_1-ATPase is a molecular motor in which the γ subunit rotates inside the $\alpha_3\beta_3$ ring upon adenosine triphosphate (ATP) hydrolysis. Recent works on single-molecule manipulation of F_1-ATPase have shown that kinetic parameters such as the on-rate of ATP and the off-rate of adenosine diphosphate (ADP) strongly depend on the rotary angle of the γ subunit (Hirono-Hara et al. 2005; Iko et al. 2009). These findings provide important insight into how individual reaction steps release energy to power F_1 and also have implications regarding ATP synthesis and how reaction steps are reversed upon reverse rotation. An important issue regarding the angular dependence of kinetic parameters is that the angular position of a magnetic bead rotation probe could be larger than the actual position of the γ subunit due to the torsional elasticity of the system. In the present study, we assessed the stiffness of two different portions of F_1 from thermophilic *Bacillus* PS3: the internal part of the γ subunit embedded in the $\alpha_3\beta_3$ ring, and the complex of the external part of the γ subunit and the $\alpha_3\beta_3$ ring (and streptavidin and magnetic bead), by comparing rotational fluctuations before and after cross-linkage between the rotor and stator. The torsional stiffnesses of the internal and remaining parts were determined to be around 223 and 73 pNnm/radian, respectively. Based on these values, it was estimated that the actual angular position of the internal part of the γ subunit is one-fourth of the magnetic bead position upon stalling using an external magnetic field. The estimated elasticity also partially explains the accommodation of the intrinsic step size mismatch between F_o and F_1-ATPase.

Keywords F_1-ATPase · Hybrid F_1 · Crosslink · γ-Subunit · Stiffness

Introduction

F_oF_1-ATP synthase, which is found in thylakoid membrane, mitochondrial inner membrane, and bacterial membrane, catalyzes ATP synthesis from ADP and inorganic phosphate (P_i) coupled with proton flow down the proton motive force (pmf) across the membrane (Yoshida et al. 2001). This enzyme consists of two rotary motors, F_o and F_1, driven by pmf and ATP hydrolysis, respectively. F_1 is composed of $\alpha_3\beta_3\gamma\delta\varepsilon$ subunits in bacterial types, and the minimum complex forming a motor is the $\alpha_3\beta_3\gamma$ subcomplex. The α and β subunits, bearing the noncatalytic and catalytic site, respectively, form the hexameric stator ring by aligning alternately. The rotary shaft is the γ subunit, which is inserted into the $\alpha_3\beta_3$ ring. By hydrolyzing ATP, F_1 rotates the γ subunit counterclockwise against the $\alpha_3\beta_3$ ring when viewed from the membrane side (Noji et al. 1997). On the other hand, F_o is composed of $ab_2c_{10\sim15}$ subunits. The c subunits align in a circle to form a ring complex, and the combination of the c-ring with the ab_2 subunits forms a proton channel. The c-ring rotates against the ab_2 subunits upon proton flow. In the whole complex of ATP synthase, F_o and F_1 are connected through central (γ, ε, and c subunits) and peripheral (δ and b subunits) stalks. Under physiological condition with sufficient pmf, F_o generates larger torque than F_1 and forcibly rotates the γ subunit

Electronic supplementary material The online version of this article (doi:10.1007/s00249-010-0616-9) contains supplementary material, which is available to authorized users.

D. Okuno · R. Iino · H. Noji (✉)
The Institute of Scientific and Industrial Research,
Osaka University, Mihogaoka 8-1,
Ibaraki, Osaka 567-0047, Japan
e-mail: hnoji@sanken.osaka-u.ac.jp

Published online: 13 June 2010

clockwise, leading the reverse reaction of ATP hydrolysis, i.e., ATP synthesis on F_1. When the pmf is small, F_1 rotates the c-ring of F_o to pump protons to generate pmf.

F_1 carries out a 120° step rotation upon one ATP hydrolysis reaction (Yasuda et al. 1998). This 120° step was further resolved into two substeps of 80° and 40°, respectively, by laser dark-field microscopy imaging (Yasuda et al. 2001). The dwell before the 80° substep is inversely proportional to [ATP] and thus was identified as the ATP waiting state. The 40° substep is triggered after at least two reaction steps, one of which was identified as hydrolysis by using a mutant F_1 with a slow ATP hydrolysis rate, $F_1(\beta$E190D), and a slowly hydrolyzed ATP analogue, adenosine-5′-(γ-thio)triphosphate (ATPγS) (Shimabukuro et al. 2003). Thereby, the dwells before the 80° and 40° substeps are referred to as the binding dwell and the catalytic dwell, respectively. The study of a hybrid F_1 carrying a single copy of β(E190D) revealed that β hydrolyzes ATP after the γ rotates 200° from the binding angle where the ATP bound to the β (Ariga et al. 2007). Simultaneous observation of binding/unbinding of a fluorescently labeled ATP analog with γ rotation showed that ADP is released at 240° from its binding angle. Results of the rotation assay at high [P_i] suggested that P_i is released at 200° or 320° (Adachi et al. 2007; Watanabe et al. 2008). Recently, a temperature-sensitive (TS) reaction was found in the rotation assay at low temperature (Watanabe et al. 2008). Following this finding, it was shown that the TS reaction occurs at 0° and corresponds to a conformational rearrangement before or after ATP binding (Enoki et al. 2009). Thus, F_1 has two stable conformations in the unitary step of 120°: dwelling states at the binding angle and the catalytic angle, to which all elementary reaction steps are assigned.

While F_1 has six potential minima in a turn, each 80° or 40° from its neighbors, it is thought that F_o has 10–15 potential minima, depending on the number of c subunits in the c-ring (von Ballmoos et al. 2008). Therefore, the step sizes of F_1 and F_o should be very different. Actually, it was reported that the F_o motor from *Escherichia coli* (*E. coli*) with a c_{10}-ring rotates in 36° steps in ATP synthesis condition (Duser et al. 2009). In addition, the number of c subunits is not a multiple of three in the majority of F_oF_1–ATP synthase. Thus, the gears of F_o and F_1 have an intrinsic mismatch. An important question regarding their mechanical coupling is how this intrinsic mismatch is accommodated. A feasible explanation is that some elastic portion would enable the potential minima of the motors to be matched by twisting (Junge et al. 2009; Mitome et al. 2004). Considering that the structurally thinnest part in the F_oF_1 complex is the coiled-coil region of the γ subunit in addition to the b_2 dimer, it is important to measure the elasticity of this part of the γ subunit (Sielaff et al. 2008).

The elasticity of the γ subunit is also important for interpretation of recent single-molecule manipulation works on F_1. Inhibitory ADP, which tightly binds to F_1 and blocks the catalysis, can be repelled out when inactivated F_1 is forcibly rotated (Hirono-Hara et al. 2005). From kinetic analysis of mechanical activation, it was revealed that the ADP release rate strongly depends on the rotary angle. It was also reported that the ATP binding rate increases in the forward direction, suggesting that the ATP-F_1 complex is largely stabilized upon γ rotation, releasing the binding energy through γ rotation (Iko et al. 2009). The rotary angle dependencies of kinetic parameters represent the essential features of the mechanochemical coupling mechanism of F_1. However, in these experiments, the γ orientation was monitored using magnetic beads attached to the protruding part of γ. Considering the possible elasticity of γ, it is likely that the actual angular position of the internal part of γ would be somewhat different from the angular position of the beads. Thus, it is required to determine how γ twists under external force.

There are some studies on the elasticity of the γ subunit. From the theoretical point of view, the existence of elasticity of γ was proposed for smooth torque transmission (Oster and Wang 2000; Panke and Rumberg 1999). In molecular dynamics simulation work, the γ subunit was forcibly rotated in the direction of ATP synthesis, and the distortion of the coiled-coil region of the γ subunit was observed (Ma et al. 2002). Experimental verification of such elasticity was obtained by Junge's group using F_1 or F_oF_1 derived from *E. coli* (EF_1 or EF_oF_1) (Sielaff et al. 2008). They introduced a pair of cysteine residues at the rotor–stator interfaces, i.e., the γ–β or γ–α interface in F_1 or a–c interface in F_o. A fluorescently labeled magnetic bead or actin filament was attached to the rotor part as a probe, and the rotary fluctuation of F_1 or F_oF_1 which was crosslinked at the introduced cysteine residues through the disulfide bond was measured at the single-probe level. The total stiffness of the system was determined from this fluctuation. By comparing the stiffness of F_1 crosslinked at different points, the stiffness of the internal part of system (i.e., the part of the γ subunit embedded in the $\alpha_3\beta_3$ complex), the $\gamma\varepsilon$-c-ring conjugate, or the peripheral stalk was estimated. However, there are several concerns regarding Sielaff's experiment. One is the functionality of the tested molecules, as ATP-driven rotation of the molecules was not confirmed even though only a few percent of molecules are functional in F_1 rotation assays. Another issue is the recording rate. They fixed the recording rate at 25 frames/s, but this could be too slow to follow the rotary fluctuation, which would cause overestimation of the elasticity. Thus, it is required to re-evaluate the stiffness of F_1. Another motivation for this work is to correlate the stiffness of γ with the reported angle dependency of kinetic parameters

as revealed by single-molecule manipulation work. Since F_1 from thermophilic *Bacillus* PS3 (TF_1) was used in these works, the stiffness of TF_1 was investigated in the present study.

Materials and methods

Preparation of F_1

$\alpha_3\beta_3\gamma$ subcomplex of F_1-ATPase derived from thermophilic *Bacillus* PS3 (TF_1) was used. For the rotation assay, $\alpha(His_6$ at N-terminus/C193S$)_3\beta(His_{10}$ at N-terminus$)_3\gamma$(S108C/I211C) was used as a wild-type F_1. In order to measure the torsional stiffness of the γ subunit with the β–γ crosslink, cysteine residues were introduced into γR84 or/and βE391 of wild-type F_1 and $\alpha_3\beta$(E190D)$_3\gamma$ to construct two mutants: $\alpha_3\beta_3\gamma$(R84C) and $\alpha_3\beta$(E190D/E391C)$_3\gamma$(R84C) (Okuno et al. 2008). Mutagenesis to construct the expression vectors of these mutants was performed as previously reported for β–γ crosslinking (Bandyopadhyay and Allison 2004). The mutants of F_1 were expressed in *E. coli*, purified, and biotinylated as previously reported (Rondelez et al. 2005). For reconstitution of the hybrid F_1, $\alpha_3\beta_2\beta$(E190D/E391C)γ(R84C), protein solutions of $\alpha_3\beta_3\gamma$(R84C) and $\alpha_3\beta$(E190D/E391C)$_3\gamma$(R84C) were mixed at molar ratio of 2:1 and incubated for over 2 days in the presence of 200 mM NaCl and 100 mM dithiothreitol (DTT) at 4°C and pH 7.0 (Okuno et al. 2008).

Rotation assay

Rotation of F_1 was visualized by attaching a magnetic bead ($\sim$0.2 μm, Seradyn, Indianapolis, USA) to the γ subunit of F_1 and immobilizing the $\alpha_3\beta_3$ ring on a nickel-nitrilotriacetic acid (Ni–NTA)-modified glass surface. Phase-contrast images of the rotating bead were obtained with the combination of an inverted optical microscope (IX-70 or 71; Olympus, Tokyo) and a 100× objective lens, equipped with magnetic tweezers (Hirono-Hara et al. 2005). Images were recorded using a high-speed camera (FASTCAM, 1024CPI; Photron, USA or HAS220, DETECT; Tokyo) at 60–3,000 frames/s. For measurement of the thermal fluctuation, the recording rate was fixed at 1,000 frames/s. The recorded images were analyzed using a custom-made plug-in for ImageJ software (K. Adachi; Gakushuin University). The experimental procedures of the rotation assay were almost the same as previously reported (Okuno et al. 2008). In the case of recording rate dependency of σ at the ATP binding dwell position, the buffer composition was 50 mM 3-(*N*-morpholino)propanesulfonic acid (MOPS)-KOH at pH 7.0, 50 mM KCl, 60 nM ATP, 1 mM phospho(enol)pyruvate, 0.1 mg/mL pyruvate kinase, and 5 mg/mL bovine serum albumin (BSA). To measure the measurement system error, the buffer consisted of 5 mM 4-(2-hydroxyethyl)-1-piperazine ethanesulfonic acid (HEPES)–KOH at 8.0, 5 mM KCl, 200 nM ATP, 2 mM $MgCl_2$, and 100 μM $CuCl_2$. For β–γ crosslink experiments, the content of buffer was different. The basal buffer for the rotation assay (before crosslinking and after washing) was 50 mM HEPES–KOH at pH 8.0, 50 mM KCl, 200 nM ATP, 2 mM $MgCl_2$, 1 mM phospho(enol)pyruvate, 0.1 mg/mL pyruvate kinase, 5 mg/mL BSA, and 1 mM DTT. For β–γ crosslinking, 200 μM 5,5′-dithiobis(2-nitrobenzoic acid) (DTNB) was added to the basal buffer, from which DTT and BSA were omitted to avoid consumption of DTNB.

Results

Experimental system for stiffness measurement

In order to measure the stiffness of the γ subunit in TF_1, we employed mostly the same experimental procedures as in former work (Sielaff et al. 2008). However, here we focused on only actively rotating molecule to avoid the adverse effect of nonfunctional molecules. We also assessed the effect of recording rate on the measurements. Figure 1 shows a schematic of the experimental system. The $\alpha_3\beta_3\gamma$ subcomplex of TF_1 was fixed on the Ni–NTA-modified glass surface through interaction between His-tag and Ni^{2+}-NTA. A magnetic bead ($\sim$0.2 μm) was attached onto the protruding part of γ using streptavidin–biotin to visualize the motion. Supposing that dwelling F_1 is in thermal equilibrium, the torsion stiffness of the system, κ, is determined from the principle of equipartition of energy:

$$1/2\kappa\sigma^2 = 1/2k_BT, \quad (1)$$

where k_B is the Boltzmann constant, T is absolute temperature, and σ is the standard deviation of the angular position of the bead. Here, we consider the system in two parts: the internal part of γ, and the complex of the external portion of γ and the $\alpha_3\beta_3$ ring (and streptavidin and magnetic bead). To resolve the total stiffness (κ^{total}) into two parts, we introduced crosslinkage at the boundary of these parts, using which the stiffness of the system except for the internal part, $\kappa^{crosslink}$, was measured. Because these compliant parts are connected in tandem, the internal stiffness, $\kappa^{internal}$, was determined from the following equation:

$$1/\kappa^{total} = 1/\kappa^{internal} + 1/\kappa^{crosslink}. \quad (2)$$

Recording rate versus σ

Each video image is averaged over the exposure time of recording. Therefore, in order to measure the stiffness from the existence probability of a Brownian particle, one has to

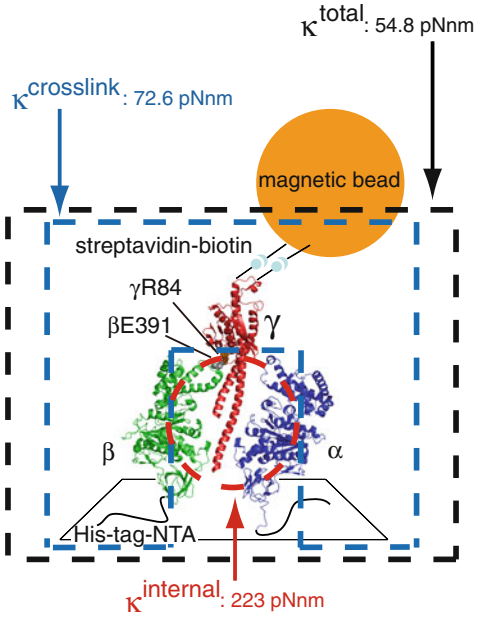

Fig. 1 Schematic of the experimental setup for measuring the thermal fluctuation of the γ subunit of F_1-ATPase and summary of the stiffnesses of several parts from this study. F_1-ATPase was fixed onto the surface of a Ni–NTA-modified cover slip through interaction between Ni^{2+} and His-tag. The probe for visualization was attached to the protruding part of the γ subunit. In this experiment, a magnetic bead was used as a probe. Cys residues were introduced into βE391 and γR84 of TF_1 to make a disulfide bond between theses residues. Only one α and β subunit of $\alpha_3\beta_3$ ring are shown. The parts fenced by *black* and *blue dotted* lines correspond to total stiffness (κ^{total}) and the stiffness of the system except for the internal part of the γ subunit as determined from crosslinked F_1 ($\kappa^{crosslink}$), respectively. The circular part with *red dotted line* corresponds to the internal stiffness ($\kappa^{internal}$) as determined from κ^{total} and $\kappa^{crosslink}$. The structural model was generated using PyMOL software

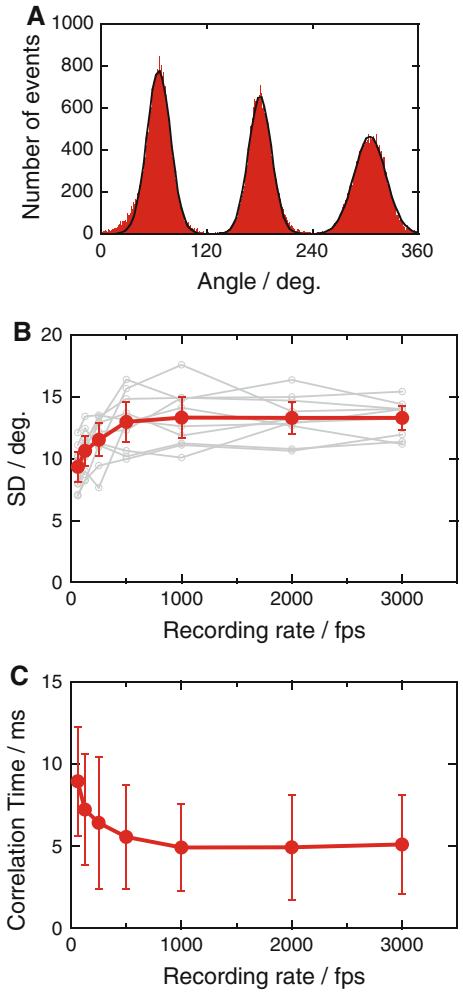

Fig. 2 Effect of recording rate on the standard deviation of rotary fluctuation in ATP binding dwell. **a** Histogram of angle distribution of rotation of F_1-ATPase at 60 nM ATP. *Black line* is the fitting curve with the combination of three Gaussian fitting curves for each ATP binding dwell pause. **b** Standard deviation (SD) of angular position during ATP binding dwell at 60 nM ATP as a function of recording rate. *Light gray* and *red circles* represent the SD of individual molecules and the average ($N = 10$). **c** Correlation time of the rotary fluctuation during ATP binding dwell and recording rate. The plots show averaged correlation times obtained by fitting the power spectra of ATP binding dwells using a Lorentzian curve of the form $A/[1 + (2\pi\tau_0 f)^2]$, where A is the power density at 0 Hz, f is the frequency, and τ_0 is the correlation time from Fig. 2 for $N = 111$–141 (ten molecules). An example power spectrum obtained at 3,000 frames/s is shown in the Supplemental Figure

record the particle position with high temporal resolution, otherwise the obtained distribution of existence probability would converge to the median, giving a higher value of stiffness than the actual value. We first examined how the recording rate affects the standard deviation (σ) of the angular position of a bead ($\phi = \sim 0.2$ μm) attached to a F_1 molecule in dwell state. Stepping rotation of F_1 was observed at an ATP-limiting condition, 60 nM, where F_1 pauses for ATP binding for 1 s on average. The histogram of angular position obtained from the stepping rotation showed three distinct peaks, each corresponding to an ATP binding dwell angle (Fig. 2a). Each peak was fitted well with a Gaussian distribution to determine σ during the ATP binding dwell. For individual molecules ($N = 10$), σ was measured at different recording rates from 60 to 3,000 frames/s (open circles in Fig. 2b). Although each molecule gave different values of σ ranging from 7.0° to 17.6°, it is clear that σ increased with recording rate and reached a plateau at 500–1,000 frames/s. The average σ increased from 9.3° to 13.3° (red circles in Fig. 2b). Thus, it appears that recording rate faster than 500 frames/s is required for precise measurement of stiffness. Although the required recording rate could be different depending on the stiffness of the sample, the actual values of σ for the catalytic dwell and crosslinked condition were around 15°, comparable to that for ATP binding (see below). We also analyzed the correlation time of the rotary fluctuation at each recording rate (Fig. 2c and Supplemental Figure). The correlation time became smaller with increasing recording

rate, converging at around 5 ms for higher than 1,000 frames/s, consistent with the result above. Therefore, we recorded the rotary fluctuation at 1,000 frames/s in subsequent experiments.

Estimation of measurement error in image analysis

We also investigated the measurement error in the image capture and analysis. First, we determined the rotational radius of magnetic beads in ATP-driven rotation or rotation forced using magnetic tweezers (red circles in Fig. 3). Then, the rotating particles were immobilized on the coverslip by infusing buffer containing 100 μM $CuCl_2$, which causes nonspecific immobilization of beads on the coverslip (blue circles in Fig. 3). The beads were immediately stuck after buffer infusion. The average σ (mean ± SD) of immobilized beads was 0.48 ± 0.28° (molecules = 11). Although the measurement error was mostly negligible, the torsional stiffness was, hereafter, corrected for the measurement system error.

Measurement of torsional stiffness of γ subunit

A hybrid F_1, $\alpha_3\beta_2\beta$(E190D/E391C)γ(R84C) (Okuno et al. 2008), was employed in this experiment. The hybrid F_1 contained a single copy of β(E190D/E391C) (Fig. 4a). E190D mutation was introduced as a position marker of the mutant β; this mutation causes a characteristic long pause of ~320 ms due to slow catalysis (Shimabukuro et al. 2003), allowing us to identify the angular position of the catalytic pause of the mutant β under microscopy. βE391C and γR84C were introduced to form a disulfide bond at the intersection of the β–γ interface and the boundary between the protruding part and the internal part of γ (Fig. 1 and 4a). Under ATP-limited condition, the hybrid F_1 exhibited asymmetric stepping rotation with ATP waiting pauses at three ATP binding angles and one hydrolysis dwell for a position of the mutant β of 200° from the ATP binding angle of mutant β in Fig. 4b (Ariga et al. 2007). Most molecules showed the expected stepping rotation with pauses at four angles. Figure 4c shows a typical histogram of the rotary angle (red), where the four angles of pauses are designated 0°, 120°, 240°, and 200°. When solution containing an oxidizing reagent, 5,5′-dithiobis(2-nitrobenzoic acid) (DTNB), was infused into the flow cell to crosslink β and γ through the disulfide bond, F_1 stopped the rotation. To confirm that the pause was not due to ADP inhibition, which also causes a pause at a catalytic angle (Hirono-Hara et al. 2001), molecules in paused state were forcibly rotated in the forward direction; F_1 in the ADP-inhibited state resumes active rotation with almost 100% efficiency when forcibly rotated over +80° for 3 s (Hirono-Hara et al. 2005). As shown in Fig. 4d, F_1 never resumed rotation even after +180° forcible rotation, verifying that the pause was due to the crosslinkage (Okuno et al. 2008). The pause position of F_1 under the oxidative condition coincided with the catalytic angle of the mutant β (Fig. 4c), consistent with previous work (Okuno et al. 2008), supporting the validity of the experiments; the differential angle of the crosslink pause from the hydrolysis pause dwell was −2.3 ± 13.1° (mean ± SD; molecules = 18, trials = 22). After measurement of the rotary fluctuation of pausing F_1, the reducing buffer was infused to release F_1 from the crosslink and to confirm that the molecule retained functionality. When the molecule did not resume rotation after reduction, the corresponding data were omitted. The catalytic pause after reduction also corresponded to the crosslink pause, the difference being only 1.0 ± 13.0° (molecules = 13, trials = 17).[1]

Each peak in the angle histograms was fitted with Gaussian curves (black and red lines in Fig. 4c) to determine σ. Average σ values (mean ± standard error, SE) for the hydrolysis dwell pause and the crosslink pause were 15.7 ± 1.0° (molecules = 18, trials = 22) and 13.6 ± 0.7° (molecules = 18, trials = 22), respectively. The average σ value for the hydrolysis dwell after reduction was 15.4 ± 1.0° (molecules = 13, trials = 17). All data are shown in the Supplemental Table. Although the values of

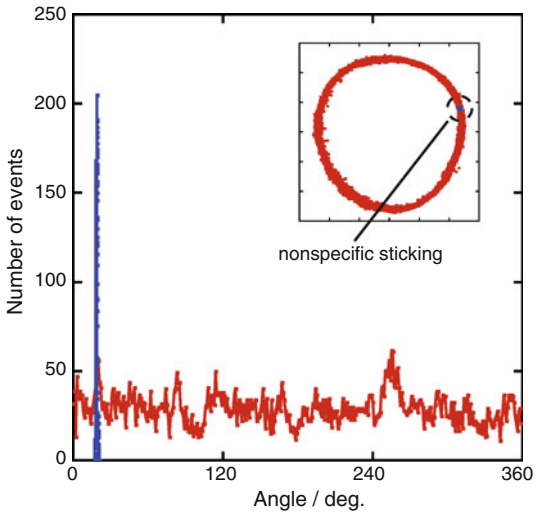

Fig. 3 Measurement error of image processing. Histogram of angle distributions of forcibly rotated (*red*) and fixed beads (*blue*) recorded at 1,000 frames/s. For this figure, the bead was forcibly rotated at constant rate (0.2 revolutions/s) using magnetic tweezers. The bead was nonspecifically fixed onto the glass by infusing buffer containing 100 μM $CuCl_2$. *Inset* shows the trace of the centroid of bead images

[1] The number of molecules after reduction is smaller than before reduction. This is because molecules whose rotation behavior, such as angle distribution or pause position, differed largely from the original ones were omitted from the data analysis.

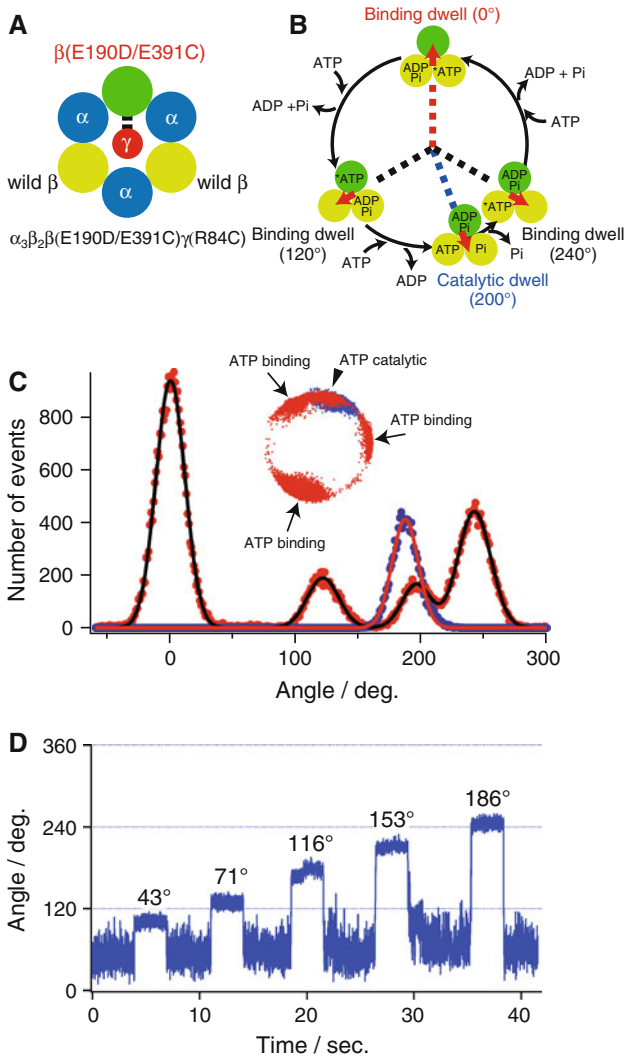

Fig. 4 Crosslinking experiment of hybrid F_1, $\alpha_3\beta_2\beta$(E190D/E391C)γ(R84C). **a** Schematic illustration of the hybrid F_1, $\alpha_3\beta_2\beta$(E190D/E391C)γ(R84C). *Short black sticks* show the cysteine residues at βE391 and γR84 to make a disulfide bond. **b** Circular reaction diagram for hybrid F_1. ATP binds to β(E190D/E391C) at 0° (*red dotted line*) and exhibits a long hydrolysis dwell at 200° due to slow hydrolysis of mutant βE190D (*blue dotted line*) (Ariga et al. 2007). At 120° and 240°, ATP binds to wild-type β subunits (*black dotted lines*). Although the hydrolysis dwells of wild-type β subunit are observed at 80° and 320°, the dwells are not resolved because they were too short (~1 ms) compared with the catalytic dwell of the mutant β. **c** Angle distributions of rotation at 200 nM ATP (*red circle*) and pause by crosslink (*blue circle*). *Black* and *red solid lines* are curves fitted using a combination of four or a single Gauss function(s). The binding position of β(E190D/E391C) was set at 0°. *Inset* shows the centroid of the bead image. *Arrows* and an *arrowhead* indicate the ATP binding and catalytic angles of hybrid F_1. (**d**) Time course of mechanical manipulation of crosslinked hybrid F_1 using magnetic tweezers. F_1 was manipulated with magnetic tweezers to stall at several angles (43–186°) for 3 s

σ were different for individual molecules, it appeared that the crosslinked F_1 provided smaller σ than before crosslinking or after reduction. The torsional stiffness of F_1 in each condition was calculated using Eq. (1) to be 54.8 ± 7.2 pNnm/radian for unlocked F_1, 72.6 ± 8.0 pNnm/radian for crosslinked F_1, and 57.0 ± 7.2 pNnm/radian for reduced F_1, respectively. According to Eq. (2), the torsional stiffness of the internal part of the γ subunit, κ^{internal}, was estimated from the differences of stiffness between the two values to be 223 ± 141 pNnm/radian (Fig. 1). When the stiffness determined from the reduced F_1 was used, the internal stiffness was determined to be 264 ± 188 pNnm/radian.

Discussion

The torsional stiffness of the whole system of F_1, κ^{total}, was determined to be 54.8 ± 7.2 pNnm/radian. By inducing a β–γ crosslink, this was successfully resolved into the stiffness of the two parts: the internal part of the γ subunit (κ^{internal} = 223 ± 141 pNnm/radian), and the complex of the protruding part of the γ subunit and the surrounding $\alpha_3\beta_3$ ring ($\kappa^{\text{crosslink}}$ = 72.6 ± 8.0 pNnm/radian). Although $\kappa^{\text{crosslink}}$ is comparable to the reported value of 68 pNnm/radian for the conjugated complex of the protruding part of the γ subunit, the ε subunit, and the c-ring (Sielaff et al. 2008), the stiffness of the internal part of the γ subunit is much more elastic than the reported value for EF_1 of 750 pNnm/radian. There are several possible explanations for this discrepancy, such as the difference in the source of F_1 and in the experimental setup. However, a main reason would be the difference in recording rate. They employed recording rate of 25 frames/s, even though the recording rate is critical for measurement of thermal fluctuation; a slow recording rate could give an apparently smaller deviation of fluctuation, providing a higher stiffness than the actual value. The exposure time of recording should be shorter than the relaxation time of the system, which is proportional to the drag coefficient. Although the drag coefficient of the rotation marker in the former study is unclear, it should be comparable to that of the present study considering that the maximum rotational velocity of F_1 carrying these probes is comparable and in the range of several turns/s. Therefore, the recording rate of the previous work, 25 frames/s, would be too slow to determine the actual rotary fluctuation.

Interestingly, the κ^{internal} value of 223 ± 141 pNnm/radian determined in this study is comparable to the value of κ^{total} (210–275 pNnm/radian) determined by recent, unprecedentedly fast imaging of TF_1 rotation with microsecond temporal resolution (Ueno et al. 2010). The sole difference in the experimental condition is the rotation marker used, being a ~0.2 μm magnetic bead in the present study and a 40 nm gold colloid for the microsecond imaging. The agreement between the two values suggests

that the apparent elasticity of the protruding part of the γ subunit found in the present study is probably caused by surface polymer conjugating the bead and streptavidin. If so, the protruding part of the γ subunit should be rigid, at least stiffer than the internal part. This contention seems to be reasonable, considering the structural features of γ; the radius of the protruding part is larger than that of the internal part, although this is opposite to the implication from the previous work that the external complex of γ, ε, and c-ring is much softer than the internal coiled coil of γ (Sielaff et al. 2008). More extensive analysis would be required to address this issue.

From the measured stiffness, the torsion angle was estimated. Under the external torque of 40 pNnm applied by F_o motor or magnetic tweezers, the internal part of γ twists $\sim 10°$ at most, which can in part relieve the asymmetry mismatch between F_o and F_1. If the torque is generated not at the bottom of the internal part of γ but at the intersection between the protruding part and the internal part (Furuike et al. 2008), the elasticity of the internal part cannot contribute to the elastic coupling of F_o and F_1. Even in the case where all of the internal region is involved in the elastic coupling, the stored elastic energy is only 4 pNnm, almost negligible compared with the total outcome of F_1 by single ATP hydrolysis of 80 pNnm. However, the situation would be drastically changed if the protruding part of γ were actually elastic; the torsional angle of the γ subunit under 40 pNnm torque is totally $\sim 42°$, which could fully relieve the asymmetric mismatch. The stored elastic energy is 15 pNnm, for a total of 30 pNnm considering the two substeps in the 120° step. Thus, the elasticity of the γ subunit might act as the elastic buffer for smooth torque transmission and resolve the symmetry mismatch despite the different gear numbers of the F_o and F_1 motors.

The stiffness of the complex of the external part of the γ subunit and the $\alpha_3\beta_3$ ring (and streptavidin and magnetic bead) proved to be three times smaller than that of the internal part. The implication of this finding for the angle dependency is that the apparent angle of the magnetic beads would be four times larger than the actual position of the internal part of the γ subunit, regardless of the rigidity of the protruding part. When the magnetic bead is rotated 10° using magnetic tweezers, the angular position of the upper contact region with β (around βE391 in Fig. 1) is around 2.5°. Therefore, the actual angle dependence would be four times higher than thought; the activation energy change of ADP release from ADP-inhibited F_1 and ATP binding should be corrected to be -29.8 k_BT/radian, and -9.2 to -6.9 k_BT/radian, respectively, (Hirono-Hara et al. 2005; Iko et al. 2009).

Acknowledgments We thank Y. Iko-Tabata and R. Hasegawa for technical assistance, W. Allison (University of California, San Diego) for plasmid vectors of mutant TF_1 from *Bacillus* PS3, K. Adachi (Gakushuin University) for the custom image analysis program, and members of the Noji laboratory for help and advice. This work was supported by a Grant-in-Aid for Scientific Research (No. 18074005 to H.N.) from the Ministry of Education, Culture, Sports, Science, and Technology of Japan.

References

Adachi K, Oiwa K, Nishizaka T, Furuike S, Noji H, Itoh H, Yoshida M, Kinosita K Jr (2007) Coupling of rotation and catalysis in F(1)-ATPase revealed by single-molecule imaging and manipulation. Cell 130:309–321. doi:10.1016/j.cell.2007.05.020

Ariga T, Muneyuki E, Yoshida M (2007) F1-ATPase rotates by an asymmetric, sequential mechanism using all three catalytic subunits. Nat Struct Mol Biol 14:841–846. doi:10.1038/nsmb1296

Bandyopadhyay S, Allison WS (2004) The ionic track in the F1-ATPase from the thermophilic Bacillus PS3. Biochemistry 43:2533–2540. doi:10.1021/bi036058i

Duser MG, Zarrabi N, Cipriano DJ, Ernst S, Glick GD, Dunn SD, Borsch M (2009) 36 degrees step size of proton-driven c-ring rotation in FoF1-ATP synthase. EMBO J 28:2689–2696. doi:10.1038/emboj.2009.213

Enoki S, Watanabe R, Iino R, Noji H (2009) Single-molecule study on the temperature-sensitive reaction of F1-ATPase with a hybrid F1 carrying a single beta(E190D). J Biol Chem 284:23169–23176. doi:10.1074/jbc.M109.026401

Furuike S, Hossain MD, Maki Y, Adachi K, Suzuki T, Kohori A, Itoh H, Yoshida M, Kinosita K Jr (2008) Axle-less F1-ATPase rotates in the correct direction. Science 319:955–958. doi:10.1126/science.1151343

Hirono-Hara Y, Noji H, Nishiura M, Muneyuki E, Hara KY, Yasuda R, Kinosita K Jr, Yoshida M (2001) Pause and rotation of F(1)-ATPase during catalysis. Proc Natl Acad Sci USA 98:13649–13654. doi:10.1073/pnas.241365698

Hirono-Hara Y, Ishizuka K, Kinosita K Jr, Yoshida M, Noji H (2005) Activation of pausing F1 motor by external force. Proc Natl Acad Sci USA 102:4288–4293. doi:10.1073/pnas.0406486102

Iko Y, Tabata KV, Sakakihara S, Nakashima T, Noji H (2009) Acceleration of the ATP-binding rate of F1-ATPase by forcible forward rotation. FEBS Lett 583:3187–3191. doi:10.1016/j.febslet.2009.08.042

Junge W, Sielaff H, Engelbrecht S (2009) Torque generation and elastic power transmission in the rotary F(O)F(1)-ATPase. Nature 459:364–370. doi:10.1038/nature08145

Ma J, Flynn TC, Cui Q, Leslie AG, Walker JE, Karplus M (2002) A dynamic analysis of the rotation mechanism for conformational change in F(1)-ATPase. Structure 10:921–931. doi:10.1016/S0969-2126(02)00789-X

Mitome N, Suzuki T, Hayashi S, Yoshida M (2004) Thermophilic ATP synthase has a decamer c-ring: indication of noninteger 10:3 H+/ATP ratio and permissive elastic coupling. Proc Natl Acad Sci USA 101:12159–12164. doi:10.1073/pnas.0403545101

Noji H, Yasuda R, Yoshida M, Kinosita K Jr (1997) Direct observation of the rotation of F1-ATPase. Nature 386:299–302. doi:10.1038/386299a0

Okuno D, Fujisawa R, Iino R, Hirono-Hara Y, Imamura H, Noji H (2008) Correlation between the conformational states of F1-ATPase as determined from its crystal structure and single-molecule rotation. Proc Natl Acad Sci USA 105:20722–20727. doi:10.1073/pnas.0805828106

Oster G, Wang H (2000) Reverse engineering a protein: the mechanochemistry of ATP synthase. Biochim Biophys Acta 1458:482–510. doi:10.1016/S0005-2728(00)00096-7

Panke O, Rumberg B (1999) Kinetic modeling of rotary CF0F1-ATP synthase: storage of elastic energy during energy transduction. Biochim Biophys Acta 1412:118–128. doi:10.1016/S0005-2728(99)00059-6

Rondelez Y, Tresset G, Nakashima T, Kato-Yamada Y, Fujita H, Takeuchi S, Noji H (2005) Highly coupled ATP synthesis by F1-ATPase single molecules. Nature 433:773–777. doi:10.1038/nature03277

Shimabukuro K, Yasuda R, Muneyuki E, Hara KY, Kinosita K Jr, Yoshida M (2003) Catalysis and rotation of F1 motor: cleavage of ATP at the catalytic site occurs in 1 ms before 40 degree substep rotation. Proc Natl Acad Sci USA 100:14731–14736. doi:10.1073/pnas.2434983100

Sielaff H, Rennekamp H, Wachter A, Xie H, Hilbers F, Feldbauer K, Dunn SD, Engelbrecht S, Junge W (2008) Domain compliance and elastic power transmission in rotary F(O)F(1)-ATPase. Proc Natl Acad Sci USA 105:17760–17765. doi:10.1073/pnas.0807683105

Ueno H, Nishikawa S, Iino R, Tabata KV, Sakakihara S, Yanagida T, Noji H (2010) Simple dark-field microscopy with nanometer spatial precision and microsecond temporal resolution. Biophys J 98:2014–2023. doi:10.1016/j.bpj.2010.01.011

von Ballmoos C, Cook GM, Dimroth P (2008) Unique rotary ATP synthase and its biological diversity. Annu Rev Biophys 37:43–64. doi:10.1146/annurev.biophys.37.032807.130018

Watanabe R, Iino R, Shimabukuro K, Yoshida M, Noji H (2008) Temperature-sensitive reaction intermediate of F1-ATPase. EMBO Rep 9:84–90. doi:10.1038/sj.embor.7401135

Yasuda R, Noji H, Kinosita K Jr, Yoshida M (1998) F1-ATPase is a highly efficient molecular motor that rotates with discrete 120 degree steps. Cell 93:1117–1124. doi:10.1016/S0092-8674(00)81456-7

Yasuda R, Noji H, Yoshida M, Kinosita K Jr, Itoh H (2001) Resolution of distinct rotational sub steps by sub millisecond kinetic analysis of F1-ATPase. Nature 410:898–904. doi:10.1038/35073513

Yoshida M, Muneyuki E, Hisabori T (2001) ATP synthase–a marvellous rotary engine of the cell. Nat Rev Mol Cell Biol 2:669–677. doi:10.1038/35089509